Vol. 46, No. 4 (2024) 695-708, DOI: 10.24874/ti.1728.07.24.10

Tribology in Industry

www.tribology.rs

RESEARCH

Case Study: Correlations Between Curve Squeal, Weather Conditions, and Traction in a Tram Loop

Martin Valena[a,*], Milan Omasta[a], Milan Klapka[a], Radovan Galas[a], Vaclav Navratil[a], Ivan Krupka[a], Martin Hartl[a]

[a]*Faculty of Mechanical Engineering, Brno University of Technology, Technicka 2896/2, 616 69 Brno, Czechia.*

Keywords:

Wheel-rail tribology
Squeal and flange noise
Portable rail tribometer
Weather conditions
Coefficient of traction

* Corresponding author:

Martin Valena
E-mail: Martin.Valena@vut.cz

Received: 31 July 2024
Revised: 31 August 2024
Accepted: 28 October 2024

A B S T R A C T

This study explores the relationship between the coefficient of traction (CoT) and squeal noise parameters on a tram line loop, focusing on the influence of weather conditions. An automatic noise module was placed near a tram loop known for noise complaints. This module distinguishes between squeal and flange noise, recording their duration, root mean square (RMS) sound pressure level, and maximum sound pressure level when a threshold in the appropriate frequency band is exceeded. Concurrently, weather conditions were monitored, and the CoT on the rail was measured using a BUT rail tribometer. The findings reveal a notable correlation between the CoT and the duration of squeal noise, while the association with sound pressure levels was less pronounced. An increase in CoT was observed with rising relative humidity, which may be attributed to increasing temperature throughout a sunny April day, while absolute humidity remained almost constant. Furthermore, noise parameters rose with higher relative humidity and showed an inverse relationship with temperature. These findings suggest that weather conditions, particularly relative humidity and temperature, influence both the CoT and noise parameters on tram lines.

1. INTRODUCTION

Rail transport is a widely used method of transporting passengers and freight, primarily due to its low energy demands and high transport capacities. However, it also has its downsides, particularly noise. The most significant contributors to the overall noise from rail transport are rolling noise, impact noise, aerodynamic noise, and curve squeal, with their contributions varying by speed [1]. Curve squeal occurs in sharp curves with a radius of 200 m or less [2] and is particularly annoying because it is louder than rolling noise and often occurs in populated areas. The negative perception of squeal noise is amplified by ground-borne vibrations, which negatively impact the quality of life [3–6]. Therefore, considerable attention is devoted to its generation and the methods of preventing or suppressing it.

Curve squeal can be divided into squeal noise and flange noise, and both are connected to instabilities in the wheel-rail contact [7].

Flange noise is generated when the wheel flange comes into contact with a gauge face of the rail [2], usually the outer leading wheel or inner trailing wheel. The broadband noise is presented at 5-10 kHz [8]. Lateral slip (also noted as creep) between the wheel tread and the top of the rail plays an essential role in generating squeal noise, also known as top-of-rail squeal. It has a strong tonal character and study [9] identified it in interval from 400 Hz to 5 kHz. It was shown that longitudinal creep also influences squeal noise, which occurs in the frequency band of 3.5–6 kHz [10]. Many parameters, such as rolling speed, angle of attack, track geometry and dynamics influence squeal and flange noises. Therefore, they are chaotic and can be predicted only with a certain probability [11–13].

The squeal noise is mainly generated by two mechanisms: mode coupling and falling friction. Mode coupling is often caused by the coupling of modal vibrations in different directions through energy flow between them [14]. The second mechanism relates to stick-slip oscillations [15], which result from the transition between the positive and negative slopes of the creep curve. At low creep, the coefficient of traction (CoT) steeply increases with creep until it reaches the coefficient of friction. This point, known as the saturation point, typically occurs around 1-2% creep. When contact exceeds this point, slipping occurs, accompanied by thermal effects at the contact [16]. As creep returns before saturation point, the contact sticks again, and the process repeats. The negative slope of the creep curve also corresponds to negative damping; when this value exceeds the positive damping of the wheel, unstable self-excited vibrations occur [15].

The coefficient of friction and the shape of the creep curve, which affect the generation of squeal noise, strongly depend on the conditions at the wheel-rail contact. Additionally, the contact surfaces may be covered by a third-body layer that alters its friction properties, which can be classified as natural or artificial. According to Berthier [17], the natural third-body layer consists solely of particles formed during rolling-sliding motion. In contrast, Meierhofer [18] includes contaminants commonly found on the rail, such as dirt, water, snow, dust, and leaves. The artificial third-body layer contains substances intentionally added to the contact, such as sand, greases, lubricants, and top-of-rail products. These top-of-rail products are used to reduce squeal noise by providing a positive creep curve and maintaining an intermediate CoT [19–21]; however, their effectiveness depends on the amount applied, particularly for oil-based products [22,23].

In addition to contaminants affecting the frictional properties of the third-body layer, weather conditions also play a significant role [24]. The effect of relative humidity (RH) on the coefficient of friction was first observed decades ago, showing a decrease in CoT with rising RH near the surface [25]. This finding has been confirmed by numerous laboratory studies [26–29], although fewer field studies have been conducted. A field study [30] directly investigates this relationship using a pendulum tribometer with a rubber pad operating under fully sliding conditions. Measurements were taken during autumn and winter at four locations with infrequent rail operations, allowing for oxidation and leaf layer formation. Overall results support the effect, as mentioned above, of RH; however, discrepancies between individual locations and days were noted.

So far, published studies investigating curve squeal typically assess sound pressure levels (SPL) or sound power levels and frequencies while overlooking other noise parameters, such as noise duration, which can also affect noise perception. Furthermore, few studies examine the influence of weather conditions on curve squeal and friction in the field. Due to many influencing factors that change over time and the track location, it is very challenging to find correlations in larger temporal or spatial scales, as was shown, e.g. in [31]. Therefore, case studies focusing on shorter timeframes and more controlled operating conditions could yield valuable insights.

This study aims to investigate the relationship between the CoT and squeal noise parameters such as sound pressure level root mean square (SPL rms), maximum sound pressure level (max SPL), and noise duration under actual conditions on a tram line loop, accounting for variations in weather. The results will provide insights into these relationships, which may

serve as baseline data for evaluating top-of-rail products regarding changes in the coefficient of friction and noise parameters following their application. A new automatic noise module was utilized to record squeal and flange noise at their typical frequencies, while the BUT rail tribometer was employed to measure CoT on the rail head.

2. MATERIALS AND METHODS

2.1 Design of the Field Study

This field study adopts the form of a case study, in which correlations between noise, weather conditions and CoT are sought for a selected tram loop over a specified period. This work was carried out in multiple phases, as shown in Fig. 1. The main study involving the measurement of CoT took place on one sunny day at the end of April. This paper presents mainly the results from this phase of measurement. This day was preceded by a long period during which noise and weather conditions were monitored using an automatic noise module. During this phase, the noise module settings were optimised to allow independent quantification of squeal and flange noise based on analysis in the frequency domain. Various operational and external factors potentially affecting curving noise were explored. The first phase was implementing and calibrating the noise module using a standard Class I noise measurement setting.

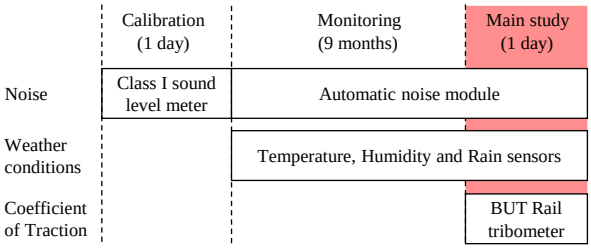

Fig. 1. Design of the field study.

2.2 Vehicle, track and operation parameters

The study was carried out on a tram loop in the northwest part of Brno, Czechia, where the curve squeal occurred frequently and impacted the people living in the surroundings. The entry curve with a radius of 21 m is placed on a low-traffic road, as shown in Fig. 2. There is one-way traffic on the line, and after passing through the curve, the trams stop at a stop. The loop consists of two parallel tracks: the inner track was used for scheduled traffic during the study, while unscheduled journeys took place on the outer track. The grooved rail with an NT1 profile was commonly worn at the top and in the groove.

During the main study, the tram line was operated by a single vehicle, Tatra KT8D5, at 15-minute intervals, from 4:45 to 22:45. Entering speed was limited to 15 km/s. The tram is bi-directional and consists of three body sections connected by joints and thus can rotate each other in all directions. The body sections are mounted on four pivoting bogies (two internal and two external), each fitted with two powered wheel sets.

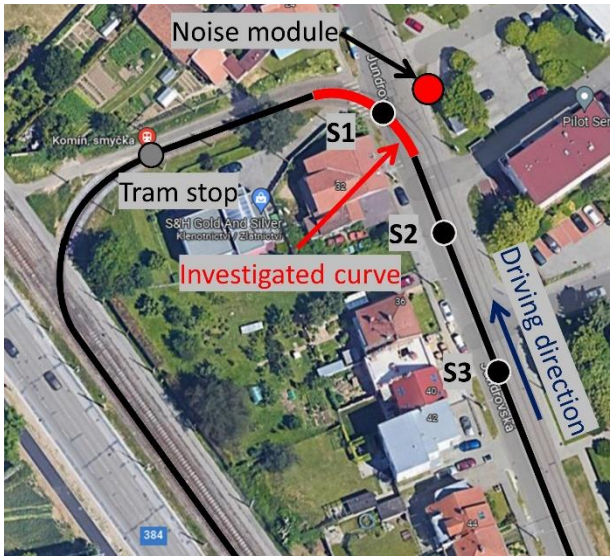

Fig. 2. Investigated tram loop.

2.3 Assessment of traction conditions

The study utilised the BUT Rail Tribometer (Fig. 3) to evaluate the creep curve and CoT [32]. The BUT Rail Tribometer consists of a measuring module and a linear guide with magnetic bases that fix the tribometer to the rail. Creep is induced by adjusting the braking torque on the wheel during the measuring pass and a torque transducer simultaneously records this torque. The tangential wheel speed and longitudinal speed are measured using encoders, which are then used to compute creep. The weight of the measuring module creates a contact pressure set to 0.9 GPa, corresponding to light-rail vehicle conditions. The BUT Rail Tribometer can be operated in three modes; for this study, the ramp mode was

chosen, where the braking torque increases in several steps. The measuring wheel was cleaned with dry tissue before the first measuring pass and was not cleaned anymore.

Fig. 3. The BUT Rail Tribometer.

Each measuring series counted 12 passes of the measuring module, performed in both directions (6 in each direction), but only the last few reached higher creep. Therefore, the resulting creep curve is composed of all these passes, which may be further fitted by a model of creep curve, see Fig. 4. The CoT was computed using the median method in creep interval from 5% to 15% [32], where the saturation point should occur. These values reliably separate points in the initial steep part of the curve and provide enough points to calculate the median CoT. It should be noted that the point scatter in the low creep regime is attributed to the finite resolution of the encoders. This occurs because of slight differences between the tangential wheel speed and longitudinal speed, which can alternate between positive and negative values.

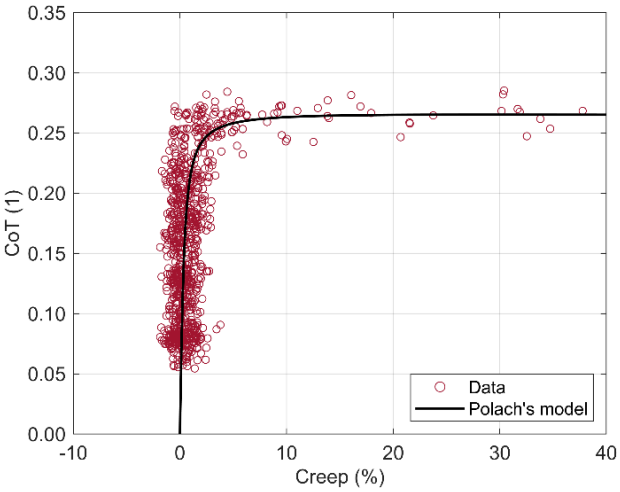

Fig. 4. Creep curve fitted by Polach's model.

Main experiment: Three measurement spots, S1 – S3, were determined on the inner track at a distance of 30 m from each other, and measurement was carried out on both rails to record any differences between the inner and the outer rail. The measurement started at 7:30, repeated approximately every hour, and ended before 16:00. A total of 48 measuring series were performed from 7:30 to 16:00 (3 spots, 2 rails and 8 times). It should be emphasized that a tram passed through that location several times between each series of measurements taken at the same spot.

Reference experiment: Two measurements were conducted as the first and last measurement series of the day on the outer track at the location corresponding to S1 on the inner track. Since the outer track was not intended for use during the main study, it can be referred to as non-operated in the context of timetable traffic on the inner track. This experiment is designed solely for comparison purposes, aiming to determine whether tram operations or changes in weather conditions have a more significant effect.

2.4 Noise measurement and its evaluation

In the first phase, calibration measurements were performed to determine the frequency bands in which squeal and flange noise is pronounced on this curve. The Svantek 977 sound level meter, equipped with an MK 255 microphone and an SV 12L preamplifier, was used to record noise data from 20 Hz to 20 kHz without weighting. The microphone was positioned 1.2 m above track level next to the pole, where the noise module should be installed. A total of 10 passes were recorded and further analysed. In addition to the measurements, the subjective impression of the pass was also noted, whether it was squeal or flange noise and how severe it was. It helped to detect the correct frequencies.

The noise module was employed for autonomous long-term noise monitoring. It was placed on the pole at a distance of 11 m from the curve and a height of 4 m, see Fig. 2. It consists of a programmable logic controller with a vibration measurement module to which an IEPE outdoor microphone is connected. The noise module is equipped with temperature, humidity, and rain sensors. It is powered by a battery. The noise module performs real-time FFT analysis,

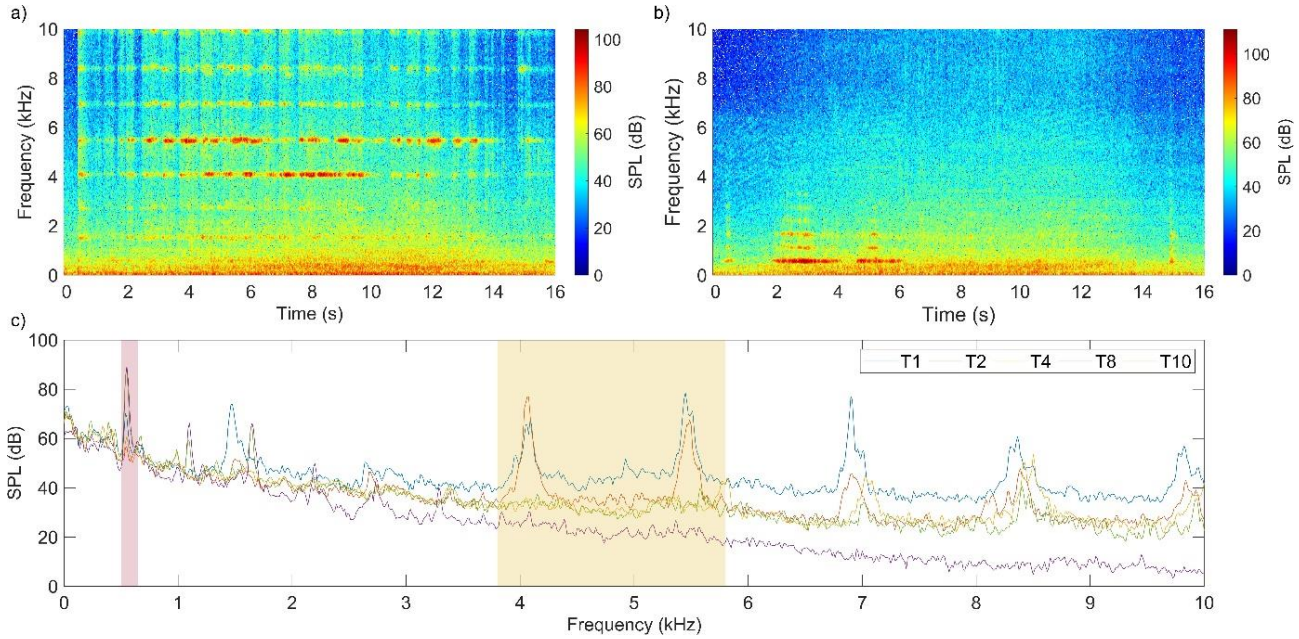

Fig. 5. Spectrograms of flange noise(a), squeal noise (b) and frequency analysis of tram passes with highlighted squeal and flange noise bands (c).

distinguishing between frequency bands characterising squeal and flange noise. Acoustic pressure was evaluated in the following frequency bands derived from preliminary measurement, the results of which are further described in chap. 3.1:

- Squeal noise: 500 – 650 Hz,
- Flange noise: 3800 – 5800 Hz.

The record in each band was created only when a threshold value was exceeded and simultaneously the noise duration was above 0.3 seconds. The threshold was set to 60 dB for squeal noise and 50 dB for flange noise. These values are high enough to suppress other noise sources, such as cars, and low enough to get a record of most tram passes. The record contains SPL rms, max SPL and noise duration. Besides acoustic parameters, the noise module records weather conditions (temperature, RH, and rain) every minute.

A single tram pass typically includes multiple noise records, as shown in Fig. 5a and b. Usually, the squeal noise is emitted intermittently as the tram wheels pass the critical points on the track where the conditions for squealing are met. The objective was to create a single record that characterizes the tram pass. The total noise duration, referred to as "duration," is calculated by summing the durations of individual records (hereinafter partial durations) during one pass. The maximum Max SPL is the highest value among the individual maximum SPLs recorded. Additionally, the SPL rms is computed using the root mean square of the individual SPL rms values. Each record is associated with a tram ID detected by a switch reading device before entering the loop.

3. RESULTS AND DISCUSSION

3.1 Definition of noise bands

The records from the first phase were analysed using FFT analysis, and the results are plotted in Fig. 5. An example of a spectrogram from the second tram pass is shown in Fig. 5a, where severe flange noise is pronounced at several higher frequencies, which is typical. The most significant frequencies are 4100 and 5500 Hz, but two lower are also essential to define correct band edges because these frequencies are exited only when flange noise is presented. In contrast, b) shows a tram pass (eighth) without any flange noise but with significant squeal noise pronounced twice between the second and sixth second of the pass. The main frequency peak is 550 Hz, but multiples up to 3300 Hz are visible, while the first three are well distinguishable. It is evident from a) and b) that the squeal and flange noise is not continuously generated during the curve

negotiation but instead emitted multiple times with short partial durations, especially the flange noise. The comparison of passes in the frequency domain is shown in c), where the typical frequencies can be seen. For clarity, only a few passes are shown.

A typical frequency of 550 Hz was observed in all cases where squeal noise occurred; therefore, the band of 500-650 Hz was chosen, which is sufficient to cover this peak (see Fig. 5c for the first highlighted area). If the upper limit is higher to include multiples, a false record of squeal noise could occur, as the peak around 1500 Hz is present when flange noise is detected. The lower limit of the flange noise was set at 3800 Hz because it reliably separates the squeal noise's last peaks while capturing the flange noise's first peaks. The upper limit of 5800 Hz is determined by noise module sampling frequency and Nyquist's theorem. The band for flange noise is highlighted in Fig. 5c, the second area. It would be better to set the upper limit higher to capture more peaks, but it might cause some difficulties with setting the SPL threshold because the SPL rms is evaluated and weak peaks might not be noticed.

3.2 Effect of weather conditions on noise

Fig. 6a and b show the typical development of noise parameters (max SPL, SPL rms and duration) corresponding to a long-term measurement, and c) weather conditions (RH, absolute humidity (AH) and temperature) recorded over the entire day. Several tram passes were silent without exceeding the thresholds; thus, the noise module could not record them, resulting in gaps in the noise records. In the case of squeal noise, max SPL and SPL rms vary around 90 and 70 dB, respectively, but neither report any noticeable trend during the day. On the other hand, the duration is longer in the morning, then decreases and increases again in the evening, which copies the development of RH over the day and has an opposite course as temperature. Similar developments can also be found in flange noise, but the main difference is that the max SPL has the same progress as the duration while the SPL rms varies around 55 dB. The duration is a suitable parameter for evaluating the severity of squeal noise because it is independent of how the sound propagates through the environment. However, it should be noted that the duration, as evaluated in this study, is still indirectly linked to SPL since SPL thresholds must be exceeded for the noise to be recorded.

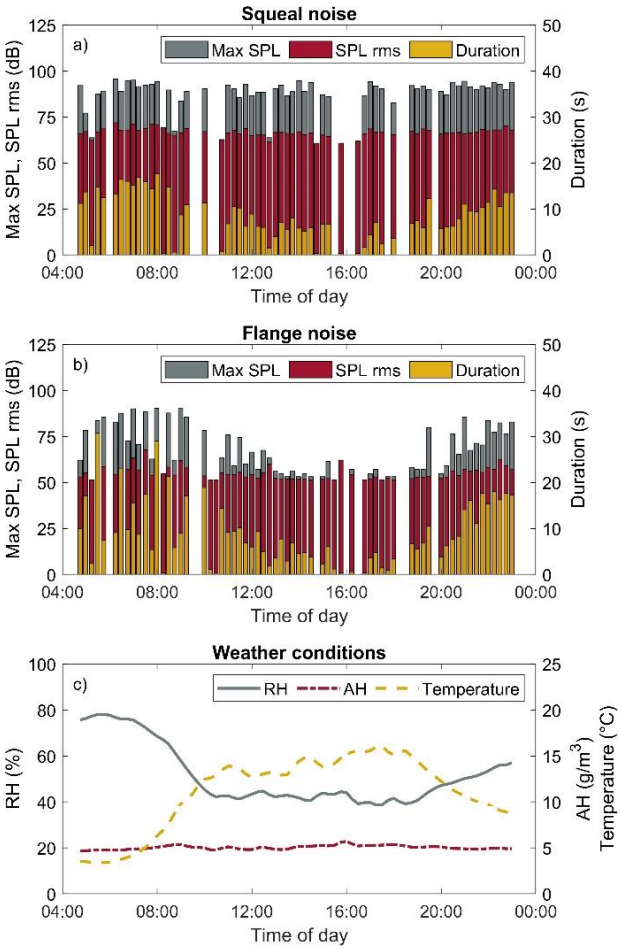

Fig. 6. Daily variation of squeal noise (a), flange noise (b), and weather conditions (c).

Parameters of squeal and flange noise are plotted in a 3D graph (Fig. 7), with temperature on the x-axis and RH on the y-axis, as these variables are interconnected. Noticeable relationships between noise parameters and weather conditions prompted a regression analysis, with Pearson correlation coefficients for squeal and flange noise presented in Table 1 and Table 2, respectively. Fig. 7a and b illustrate a clear trend: squeal duration and SPL rms decrease with lower RH and higher temperatures, while maximum SPL does not show a significant trend. The regression analysis identified the strongest correlation for squeal duration. A few points with noticeably lower values for squeal duration and maximum SPL can be observed in Fig. 7a and c; their positions in the temperature-RH plane suggest they

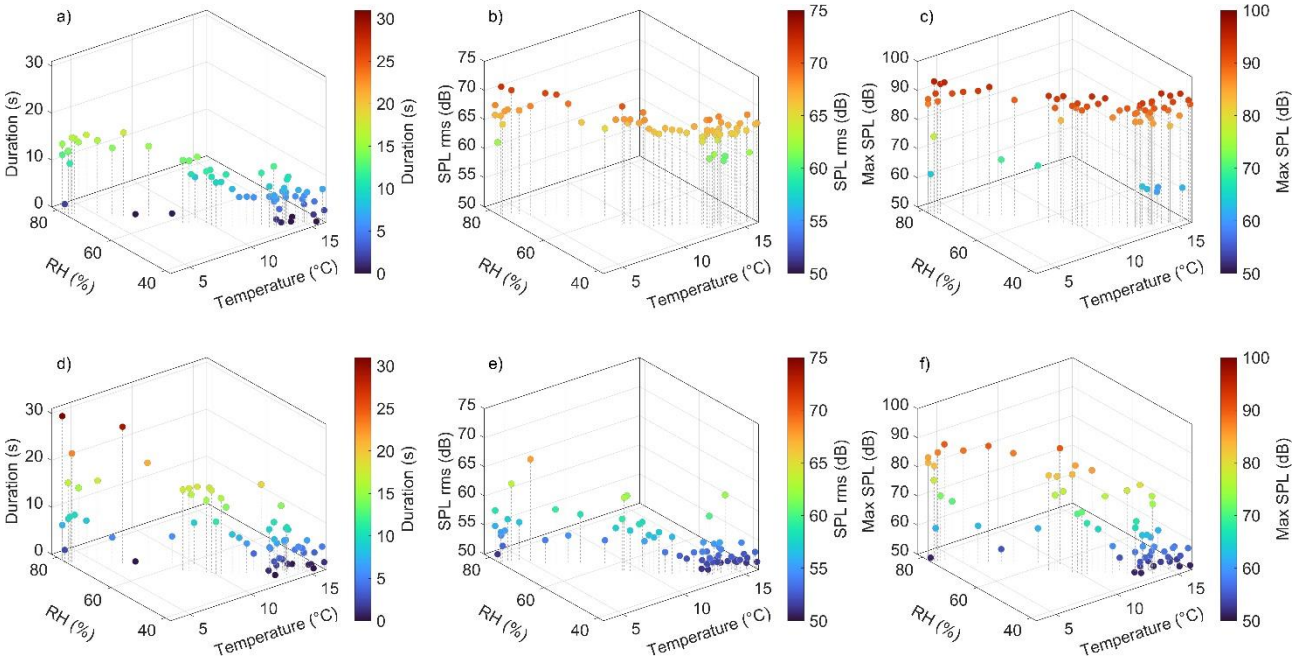

Fig. 7. The effect of temperature and RH on squeal duration (a), SPL rms of squeal noise (b), Max SPL of squeal noise (c), duration of flange noise (d), SPL rms of flange noise (e), Max SPL of flange noise (f).

correspond to each other and were recorded during the same tram passes, indicating that these passes were relatively silent and only slightly exceeded the SPL threshold. In contrast, flange noise parameters exhibit significant variability at lower or higher RH levels, with this scatter diminishing as temperature rises and RH falls (Fig. 7d-f). This indicates that higher RH or lower temperatures produce elevated noise parameters. While general trends are similar to those observed in squeal noise, the most significant correlation for flange noise was found with maximum SPL. The regression analysis shows that temperature and RH affect both squeal and flange noise, but AH has a limited impact. Most relationships are statistically significant at a 95% confidence level, although the slopes of some relationships (marked in red) may be zero.

Table 1. Pearson correlation coefficients for squeal noise (p-values in brackets)

	Temperature (°C)	RH (%)	AH (g/m³)
Duration (s)	-0.663 (<0.001)	0.626 (<0.001)	-0.506 (<0.001)
SPL rms (dB)	-0.440 (<0.001)	0.419 (<0.001)	-0.315 (0.013)
Max SPL (dB)	-0.107 (0.409)	0.061 (0.638)	-0.291 (0.022)

Increasing temperature is likely to reduce all noise parameters, as demonstrated by Maly et al. [33]. They conducted long-term measurements, recording approximately 20,000 suburban train passes under various weather conditions. Their evaluation of sound power levels showed a trend similar to that of the SPL used in this study, differing only in magnitude. Additionally, they analysed the frequency of occurrence, which exhibited the same dependency as SPL. The frequency of occurrence can be compared to the duration assessed in this study. A higher frequency of occurrence suggests that contact is more likely to produce squeal noise. Consequently, it is more probable that squeal noise will be emitted multiple times during a curve pass, leading to a longer duration. Both duration and frequency of occurrence show similar dependencies on temperature.

Table 2. Pearson correlation coefficients for flange noise (p-values in brackets)

	Temperature (°C)	RH (%)	AH (g/m³)
Duration (s)	-0.554 (<0.001)	0.511 (<0.001)	-0.368 (0.003)
SPL rms (dB)	-0.483 (<0.001)	0.481 (<0.001)	-0.067 (0.598)
Max SPL (dB)	-0.617 (<0.001)	0.593 (<0.001)	-0.272 (0.028)

The correlation coefficient between noise parameters and RH is slightly lower than that of temperature. However, the main difference is the opposite slope, meaning that all noise

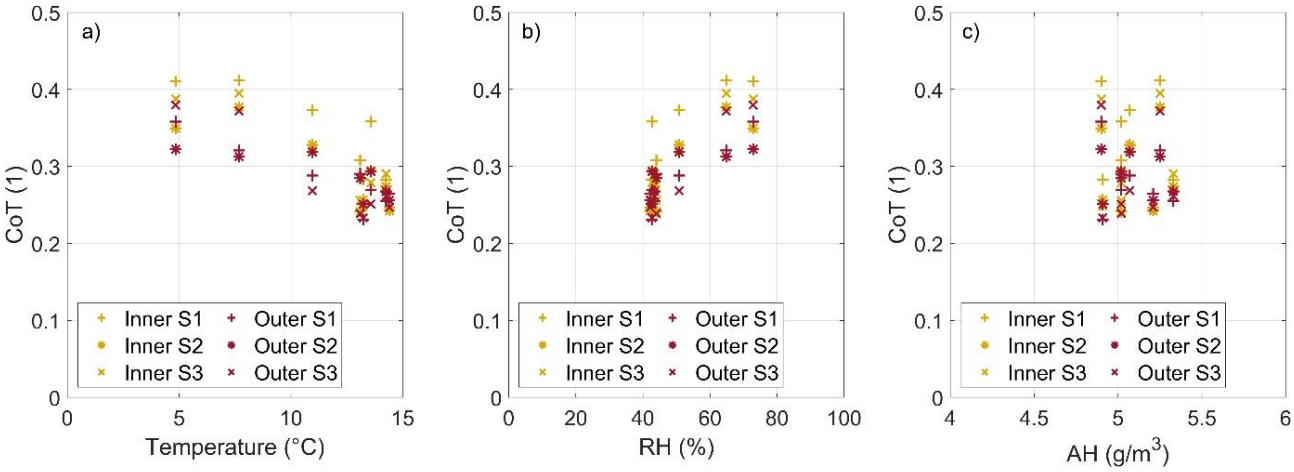

Fig. 8. The influence of weather conditions on CoT: temperature (a), RH (b) and AH (c).

parameters increase with increasing RH. This finding is consistent with a previous field study [33]. It should be noted that, according to the mentioned study, the trend also depends on the rail temperature. When the temperature is above 0 °C, the SPL increases with rising RH; when it is below 0 °C, the effect is opposite. The rail temperature was estimated to be between 0 – 10 °C based on the ambient temperature. The squeal duration can be used to compare the measured data with the publication in which the increasing probability of the squeal with increasing RH was assessed [12]. As mentioned earlier, a higher likelihood should result in a longer squeal duration, indicating that the measurement is consistent with the study [12]. Only a correlation with squeal duration was found for AH, which may be due to the limited range of AH, as the measurement was performed on a sunny day. AH varied during April between 2.77 and 11.43 g/m^3, while it reached the local minimum on the day of measurement. In this context, it might be considered as constant.

3.3 Effect of weather conditions on CoT

The friction properties of 3rd body layer presented on the rail vary with RH and temperature, as shown in Fig. 8. The colours of the points represent the inner or outer rail, and different symbols indicate the measurement place (S1-S3). Both temperature and RH significantly correlate with CoT (Table 3), although they have distinct slopes. Specifically, increasing temperatures negatively affect the CoT, while higher RH leads to an increase in CoT. In contrast, the correlation with AH is negligible, with the slope potentially being zero based on a 95% confidence interval. In all cases, the inner rail reports a higher CoT, which may be due to cleaning effect caused by the higher slip of the inner wheel while a tram negotiates the curve. A similar phenomenon was observed on the Iron Ore Line in Sweden [34] on a sunny day with an ambient temperature of 13 °C, but not under other conditions (morning dew and a frost). This was explained by different third bodies at the locations where measurements were performed, while roughness and other parameters were similar. The variation between individual spots is significant (see Fig. 8), but the overall trend remains consistent whether we consider all the data or the trend in particular spots. It may result from local friction conditions such as 3rd body layer composition, hardness, roughness and ductility [35].

The effect of temperature corresponds to findings of other papers [24,36], but the RH has an opposite effect than that described in the literature [24,26,28,30,37]. In laboratory studies, the higher RH was reached by adding steam into an enclosed chamber where the measurement was performed or using an external humidity unit. Both approaches led to an increase in AH. Besides that, experiments were carried out under constant temperature. As was mentioned before and can be seen in Fig. 8c, AH in our study is similar to the study of Zhu et al. [37]. Many field studies, for example [30] and [31], were performed in autumn under damp conditions, and the rail may be contaminated by leaves, which causes low adhesion [26]. In contrast, the presented study was performed on a regularly operated track

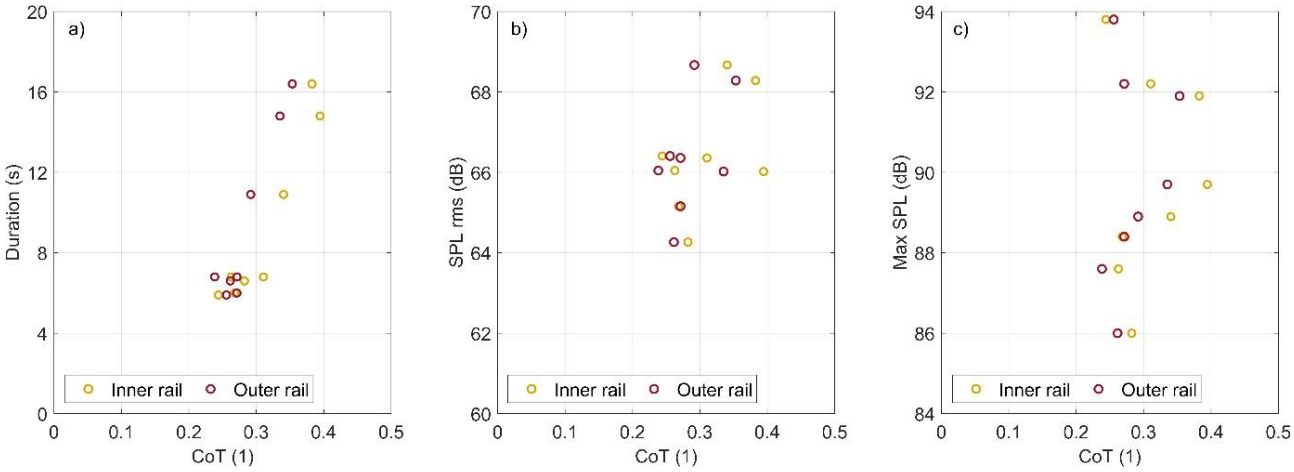

Fig. 9. The effect of CoT on squeal duration (a), SPL rms of squeal noise (b) and max SPL of squeal noise (c).

on a sunny day. The dew point fluctuated around 0 °C the previous night; however, it cannot be ruled out that some dew may have formed on the rail. Studies [37] and [38] show that haematite that increases CoT can be generated under high RH. In contrast, oxyhydroxides result from hydration [39] and decrease CoT [40]. Additionally, the wheel-rail contact operates under high pressure and a non-negligible amount of heat is generated due to wheel slip [41]. These conditions transform oxyhydroxides and iron oxides, whereas each type impacts friction differently [40]. This might explain the initial high CoT value. From another perspective, RH decreased between 6:00 and 11:00 in response to rising temperatures, which aligns with the trend observed in the CoT, as shown in Fig. 10. This suggests that direct exposure of the rail to sunlight from early morning, even before CoT measurements began, may increase the rail temperature and dry out the third body layer. Consequently, the lowest CoT values recorded in the afternoon were measured on dry rail. Therefore, it is more likely that changes in CoT are associated with temperature or daytime conditions rather than variations in RH.

The question arises as to whether the change in weather conditions or tram operations causes the change in frictional properties during the day. The highest CoT value was measured on the inner track in the morning and gradually decreased during the day, see Fig. 10. The reference experiment performed on non-operated rail also showed the highest CoT in the morning, while in the afternoon, it was lower. Based on this, it could be concluded that the change in weather conditions plays a substantial role, but creep and contact pressure should also affect the frictional properties [42]. It should be mentioned that a few trams passed on the outer track out of timetables, which might have affected the 3rd body layer similarly to the regular traffic on the inner track, where the traffic was heavier.

Table 3. Pearson correlation coefficients between CoT and weather conditions

	Pearson correlation coefficient	p-value
Temperature vs. CoT	-0.805	<0.001
RH vs. CoT	0.811	<0.001
AH vs. CoT	-0.065	0.660

Table 4. Pearson correlation coefficients between CoT and squeal noise parameters

	Pearson correlation coefficient	p-value
CoT vs. duration	0.899	<0.001
CoT vs. SPL rms	0.487	0.056
CoT vs. max SPL	0.168	0.534

3.4 Relationship between the CoT and squeal noise parameters

Combining the automatic noise module and the BUT rail tribometer enables us to investigate the relationship between squeal noise parameters and CoT. The study of the relationship between flange noise and CoT is not meaningful, as CoT was only measured at the top of the rail. Results indicate that increasing CoT increases the squeal duration and SPL rms. At the same time, the effect

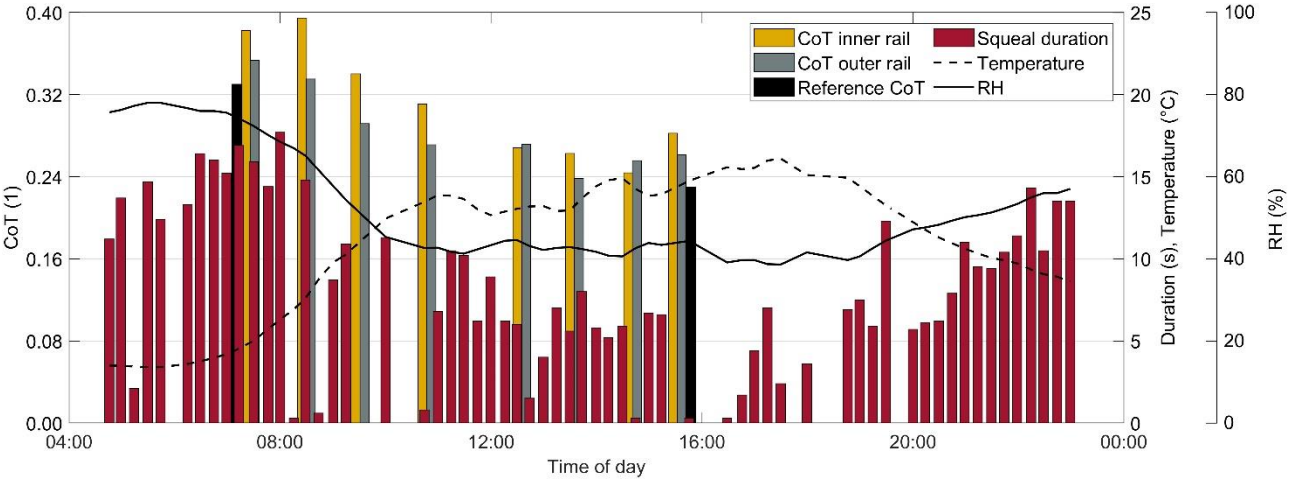

Fig. 10. Development of CoT, squeal duration and weather conditions during the daytime.

of CoT on max SPL is negligible, see Fig. 9. The correlation between squeal duration and CoT is strong and statistically significant, while the SPL rms is almost statistically significant (see Table 4), but the slope may be zero according to the 95% confidence interval. Some numerical studies have shown that the coefficient of friction affects the generation of squeal noise. The study [43] claims that a higher coefficient of friction leads to higher noise intensity, which is a similar parameter to SPL. Simultaneously, a study [44] found that a higher coefficient of friction causes the wheel-rail system to be more unstable, increasing the tendency toward squeal noise. A potential explanation for the correlation between squeal duration and CoT is that the combination of an unstable system and varying instantaneous contact conditions along the curve caused the noise to be emitted multiple times, resulting in a longer squeal duration.

Fig. 10 illustrates the development of CoT and squeal duration during the daytime, highlighting the strongest correlation observed. The CoT was lower during the day compared to the morning, and a similar trend was noted in the squeal duration; however, the squeal duration increased again in the evening. While this trend in squeal duration was evident during the monitoring phase, it does not imply that low friction cannot occur in the morning or evening. Other known mechanisms, such as forming a viscous paste made up of oxides and water [45], can also contribute to low friction conditions.

These data should be expanded to include measurements under various weather conditions to enhance knowledge. This additional data could serve as baseline curves for evaluating the effectiveness of top-of-rail products.

3.5 Limitations in the Study

This study's limitation is related to the noise measurement, which was not performed and evaluated following ISO 3095:2013. This includes the approach, device, microphone position and 3rd-octave bands. While this difference may influence the exact value of SPL, it does not change the identified trends, correlations and noise duration. In particular, this standard does not cover the distinction between squeal and flange noise, which is the main purpose of the study.

A possible limitation is that the measurement of CoT was made only in one day. The previous experiments indicate that it is difficult to obtain any correlation over a long time period due to other influences that can hardly be controlled during the tests in a real tram operation. This includes the effects of the operation of different trams with different technical conditions; maintenance interventions, weather phenomena significantly affecting the condition of the rail (leaf falls, heavy rail) and many others. Although the noise data presented were recorded in a single day, they were preceded by nine months of noise monitoring to identify typical behaviours. This pattern was also observed on the day of the CoT measurements, which started early in the morning and lasted late in the evening. To better understand the relationship between

CoT and squeal noise, measurements of CoT should be made over several days at different times of the year, and measurements should last from early morning to late evening, which is a future step.

As the tribometer's measuring wheel was cleaned by dry tissue only once before the first measurement, this might have affected the value of the CoT. The CoT characterises the contact between two bodies, while only one was being investigated. Harrison [46] showed that the condition of the measuring wheel affects the CoT due to forming a 3rd body layer on it. This layer develops with the number of passes, increasing the CoT, as observed in the study [32]. The decision not to clean the measuring wheel with a cleaning agent before each measuring series was made to better represent the actual state of a tram wheel. Despite this, the CoT gradually decreased throughout the day. Therefore, we can assume that this phenomenon did not play a significant role in this study. Moreover, the measuring wheel was visually inspected after cleaning and at the end of the day, with no changes in the running band observed. However, it can be assumed that some 3rd body layer was transferred from the rail to the wheel.

The actual values of the CoT between the wheel and rail may differ from the values measured by the tribometer. The most notable is the size difference between measuring and tram wheel, making local changes in the third body layer, roughness, and hardness more pronounced. Additionally, thermal effects in smaller contacts are less significant than in larger ones, resulting in higher CoT values. Several studies [32,47] have compared different measuring approaches and demonstrated substantial discrepancies between the results of individual methods; notably, hand-pushed portable tribometers tend to overestimate friction. Nevertheless, the BUT tribometer has been shown to give reasonable values across a range of rail conditions [32]. A more important parameter that differs between tram operation and the tribometer is speed; the tribometer operates at a speed of 0.26 m/s, and research [48] has shown that higher speeds result in lower CoT values.

4. CONCLUSION

The study examined the correlation between the CoT and curve squeal produced by a tram navigating a sharp curve. This investigation utilised both an automatic noise module and a BUT rail tribometer. The noise module could distinguish between squeal noise and flange noise using real-time frequency analysis and two pre-defined frequency bands identified in the first phase. SPL rms, max SPL and duration are recorded only when the threshold in a specific band is exceeded and the noise persists for longer than 0.3 seconds. As a result, multiple records were generated during the tram's passage through the curve, which were then processed to create a single record characterizing that specific tram pass. The noise module, in combination with data from a switch, helped to identify the noisiest trams, which were removed from the operation on this line. This improved the quality of life for residents living in the surrounding area of the tram loop as occurrence of the squeal noise was reduced.

This study presents pilot results by combining this noise module and the BUT rail tribometer. The main conclusions are as follows:

- Both squeal and flange noise parameters exhibit a negative correlation with temperature and a positive correlation with RH, while the effect of AH was not observed. The strongest correlation for squeal noise is found between squeal duration and temperature, whereas it is observed between max SPL and temperature for flange noise.
- Squeal duration shows a strong positive correlation with the CoT, while the SPL rms has a weaker correlation that is not statistically significant. Additionally, max SPL does not correlate with CoT.
- CoT decreases as temperature rises and increases with higher RH. The positive correlation between CoT and RH may be attributed to the sunny day when the temperature increased throughout the day while RH decreased. AH remained almost constant compared to the rest of the month.

Acknowledgements

This work was carried out in the framework of the projects "Josef Bozek National Center of Competence for Surface Vehicles" (TN01000026) and "Bozek Vehicle Engineering National Center of Competence" (TN02000054) that were co-financed from the state budget by the Technology Agency of the Czech Republic within the programme "National Centres of Competence".

REFERENCES

[1] R. Lewis and U. Olofsson, *Wheel-rail interface handbook*, 1st pub. Cambridge: Boca Raton: Woodhead: CRC Press, 2009.

[2] D. Thompson, *Railway Noise and Vibration*, Elsevier, 2009.

[3] A. Gidlöf-Gunnarsson, M. Ögren, T. Jerson, and E. Öhrström, "Railway noise annoyance and the importance of number of trains, ground vibration, and building situational factors," *Noise Health*, vol. 14, no. 59, pp. 190–201, Jan. 2012, doi:10.4103/1463-1741.99895.

[4] B. Griefahn, P. Bröde, A. Marks, and M. Basner, "Autonomic Arousals Related to Traffic Noise during Sleep," *Sleep*, vol. 31, no. 4, pp. 569–577, Apr. 2008, doi: 10.1093/SLEEP/31.4.569.

[5] E. Murphy and E. A. King, *Environmental Noise Pollution*, Boston: Elsevier, 2014.

[6] J. Dratva *et al.*, "Transportation Noise and Blood Pressure in a Population-Based Sample of Adults," *Environmental Health Perspectives*, vol. 120, no. 1, pp. 50–55, Sep. 2012, doi: 10.1289/ehp.1103448.

[7] P. J. Remington, "Wheel/rail squeal and impact noise: What do we know? What don't we know? Where do we go from here?," *Journal of Sound and Vibration*, vol. 116, no. 2, pp. 339–353, Jul. 1987, doi: 10.1016/S0022-460X(87)81306-8.

[8] D. T. Eadie, M. Santoro, and J. Kalousek, "Railway noise and the effect of top of rail liquid friction modifiers: changes in sound and vibration spectral distributions in curves," *Wear*, vol. 258, no. 7–8, pp. 1148–1155, Mar. 2005, doi: 10.1016/j.wear.2004.03.061.

[9] S. S. Hsu, Z. Huang, S. D. Iwnicki, D. J. Thompson, C. J. C. Jones, G. Xie, and P. D. Allen, "Experimental and theoretical investigation of railway wheel squeal," *Proceedings of the Institution of Mechanical Engineers, Part F: Journal of Rail and Rapid Transit*, vol. 221, no. 1, pp. 59–73, Jan. 2007, doi: 10.1243/0954409JRRT85.

[10] D. J. Fourie, P. J. Gräbe, P. S. Heyns, and R. D. Fröhling, "Frequency domain model for railway wheel squeal resulting from unsteady longitudinal creepage," *Journal of Sound and Vibration*, vol. 445, pp. 228–246, Apr. 2019, doi: 10.1016/j.jsv.2018.12.014.

[11] P. A. Meehan, "Investigation of chaotic instabilities in railway wheel squeal," *Nonlinear Dynamincs*, vol. 100, no. 1, pp. 159–172, Mar. 2020, doi: 10.1007/s11071-020-05493-x.

[12] X. Liu and P. A. Meehan, "Investigation of the effect of relative humidity on lateral force in rolling contact and curve squeal," *Wear*, vol. 310, no. 1–2, pp. 12–19, Feb. 2014, doi: 10.1016/j.wear.2013.11.045.

[13] Z. Yang and Z. Li, "Numerical modeling of wheel-rail squeal-exciting contact," *International Journal of Mechanical Sciences*, vol. 153–154, pp. 490–499, Feb. 2019, doi: 10.1016/j.ijmecsci.2019.02.012.

[14] N. Hoffmann, M. Fischer, R. Allgaier, and L. Gaul, "A minimal model for studying properties of the mode-coupling type instability in friction induced oscillations," *Mech. Res. Commun.*, vol. 29, no. 4, pp. 197–205, Jul. 2002, doi: 10.1016/S0093-6413(02)00254-9.

[15] D. J. Thompson, G. Squicciarini, B. Ding, and L. Baeza, "A State-of-the-Art Review of Curve Squeal Noise: Phenomena, Mechanisms, Modelling and Mitigation," *in Notes on Numerical Fluid Mechanics and Multidisciplinary Design*, vol. 139, 2018, pp. 3–41 doi: 10.1007/978-3-319-73411-8_1.

[16] O. Polach, "Creep forces in simulations of traction vehicles running on adhesion limit," *Wear*, vol. 258, no. 7–8, pp. 992–1000, Dec. 2004, doi: 10.1016/j.wear.2004.03.046.

[17] Y. Berthier, S. Descartes, M. Busquet, E. Niccolini, C. Desrayaud, L. Baillet, and M. C. Baietto-Dubourg, "The role and effects of the third body in the wheel–rail interaction," *Fatigue & Fracture of Engineering Materials & Structures*, vol. 27, no. 5, pp. 423–436, May 2004, doi: 10.1111/j.1460-2695.2004.00764.x.

[18] A. Meierhofer, C. Hardwick, R. Lewis, K. Six, and P. Dietmaier, "Third body layer-experimental results and a model describing its influence on the traction coefficient," *Wear*, vol. 314, no. 1–2, pp. 148–154, Jun. 2014, doi: 10.1016/j.wear.2013.11.040.

[19] R. Stock, L. Stanlake, C. Hardwick, M. Yu, D. Eadie, and R. Lewis, "Material concepts for top of rail friction management – Classification, characterisation and application," *Wear*, vol. 366–367, pp. 225–232, Nov. 2016, doi: 10.1016/j.wear.2016.05.028.

[20] X. Liu and P. A. Meehan, "Investigation of squeal noise under positive friction characteristics condition provided by friction modifiers," *Journal of Sound and Vibration*, vol. 371, pp. 393–405, Mar. 2016, doi: 10.1016/j.jsv.2016.02.028.

[21] D. T. Eadie, M. Santoro, and W. Powell, "Local control of noise and vibration with KELTRACK™ friction modifier and Protector® trackside application: an integrated solution," *Journal of Sound and Vibration*, vol. 267, no. 3, pp. 761–772, Oct. 2003, doi: 10.1016/S0022-460X(03)00739-9.

[22] R. Galas, M. Omasta, I. Krupka, and M. Hartl, "Laboratory investigation of ability of oil-based friction modifiers to control adhesion at wheel-rail interface," *Wear*, vol. 368–369, pp. 230–238, Dec. 2016, doi: 10.1016/j.wear.2016.09.015.

[23] R. Galas, D. Kvarda, M. Omasta, I. Krupka, and M. Hartl, "The role of constituents contained in water–based friction modifiers for top–of–rail application," *Tribology International*, vol. 117, pp. 87–97, Jan. 2018, doi: 10.1016/j.triboint.2017.08.019.

[24] S. R. Lewis, R. Lewis, U. Olofsson, D. T. Eadie, J. Cotter, and X. Lu, "Effect of humidity, temperature and railhead contamination on the performance of friction modifiers: Pin-on-disk study," *Proceedings of the Institution of Mechanical Engineers, Part F: Journal of Rail and Rapid Transit*, vol. 227, no. 2, pp. 115–127, Mar. 2013, doi: 10.1177/0954409712452239.

[25] T. M. Beagley, I. J. McEwen, and C. Pritchard, "Wheel/rail adhesion — the influence of railhead debris," *Wear*, vol. 33, no. 1, pp. 141–152, Jun. 1975, doi: 10.1016/0043-1648(75)90230-6.

[26] R. Galas, M. Omasta , L. Shi, H. Ding, W. Wang, I. Krupka, and M.Hartl, "The low adhesion problem: The effect of environmental conditions on adhesion in rolling-sliding contact," *Tribology International*, vol. 151, no. May, p. 106521, Nov. 2020, doi: 10.1016/j.triboint.2020.106521.

[27] R. Lewis, R. S. Dwyer-Joyce, U. Olofsson, J. Pombo, J. Ambrósio, M. Pereira, C. Ariaudo, and N. Kuka, "Mapping railway wheel material wear mechanisms and transitions," *Proceedings of the Institution of Mechanical Engineers, Part F: Journal of Rail and Rapid Transit,* vol. 224, no. 3, pp. 125–137, Mar. 2010, doi: 10.1243/09544097JRRT328.

[28] Y. Zhu, Y. Lyu, and U. Olofsson, "Mapping the friction between railway wheels and rails focusing on environmental conditions," *Wear*, vol. 324–325, pp. 122–128, Dec. 2014, doi: 10.1016/j.wear.2014.12.028.

[29] Y. Zhu, H. Yang, and W. Wang, "Twin-disc tests of iron oxides in dry and wet wheel–rail contacts," *Proceedings of the Institution of Mechanical Engineers, Part F: Journal of Rail and Rapid Transit*, vol. 230, no. 4, pp. 1066–1076, May 2016, doi: 10.1177/0954409715575093.

[30] M. O. Folorunso, R. Lewis, and J. L. Lanigan, "Effects of temperature and humidity on railhead friction levels," *Proceedings of the Institution of Mechanical Engineers, Part F: Journal of Rail and Rapid Transit*, vol. 237, no. 8, pp. 1009–1024, Sep. 2023, doi: 10.1177/09544097221148236.

[31] A. Meierhofer, G. Trummer, C. Bernsteiner, and K. Six, "Vehicle tests showing how the weather in autumn influences the wheel–rail traction characteristics," *Proceedings of the Institution of Mechanical Engineers, Part F: Journal of Rail and Rapid Transit*, vol. 234, no. 4, pp. 426–435, Apr. 2020, doi: 10.1177/0954409719863643.

[32] M. Valena, M. Omasta, D. Kvarda, R. Galas, I. Krupka, and M. Hartl, "An approach for the creep-curve assessment using a new rail tribometer," *Tribology International,* vol. 191, p. 109153, Mar. 2024, doi: 10.1016/j.triboint.2023.109153.

[33] T. Maly, F. Biebl, and M. Ostermann, "The effects of weather conditions and wheel wear on curve squeal," *Proceedings of the 23rd International Congress on Acoustics*, pp. 1559–1566, Sep. 2019, doi: 10.18154/RWTH-CONV-239967.

[34] S. A. Khan, J. Lundberg, and C. Stenström, "The effect of third bodies on wear and friction at the wheel-rail interface," *Proceedings of the Institution of Mechanical Engineers, Part F: Journal of Rail and Rapid Transit*, vol. 236, no. 6, pp. 662–671, Jul. 2022, doi: 10.1177/09544097211034688.

[35] J. Kalousek, D. M. Fegredo, and E. E. Laufer, "The wear resistance and worn metallography of pearlite, bainite and tempered martensite rail steel microstructures of high hardness," *Wear*, vol. 105, no. 3, pp. 199–222, Oct. 1985, doi: 10.1016/0043-1648(85)90068-7.

[36] K. S. Baek, K. Kyogoku, and T. Nakahara, "An experimental study of transient traction characteristics between rail and wheel under low slip and low speed conditions," *Wear*, vol. 265, no. 9–10, pp. 1417–1424, May 2008, doi: 10.1016/j.wear.2008.02.044.

[37] Y. Zhu, U. Olofsson, and H. Chen, "Friction Between Wheel and Rail: A Pin-On-Disc Study of Environmental Conditions and Iron Oxides," *Tribology Letters*, vol. 52, no. 2, pp. 327–339, Nov. 2013, doi: 10.1007/s11249-013-0220-0.

[38] J. L. Viesca, S. González-Cachón, A. García, R. González, A. Bernardo-Sánchez, and A. Hernández Battez, "Influence of environmental conditions and oxidation on the coefficient of friction using microalloyed rail steels," *Proceedings of the Institution of Mechanical Engineers, Part F: Journal of Rail and Rapid Transit*, vol. 235, no. 3, pp. 353–360, 2021, doi: 10.1177/0954409720925682.

[39] K. Ishizaka, S. R. Lewis, and R. Lewis, "The low adhesion problem due to leaf contamination in the wheel/rail contact: Bonding and low adhesion mechanisms," *Wear*, vol. 378–379, pp. 183–197, Feb. 2017, doi: 10.1016/j.wear.2017.02.044.

[40] B. T. White, R. Lewis, U. Olofsson, and Y. Lyu, "The Contribution of Iron Oxides to the Wet-Rail Phenomenon," *Civil-comp Proceedings*, May 2016, doi: 10.4203/ccp.110.154.

[41] M. Ertz and F. Bucher, "Improved Creep Force Model for Wheel/Rail Contact Considering Roughness and Temperature," *Vehicle System Dynamics*, vol. 37, no. sup1, pp. 314–325, Jan. 2002, doi: 10.1080/00423114.2002.11666242.

[42] E. Vollebregt, K. Six, and O. Polach, "Challenges and progress in the understanding and modelling of the wheel–rail creep forces," *Vehicle System Dynamics*, vol. 59, no. 7, pp. 1026–1068, Jul. 2021, doi: 10.1080/00423114.2021.1912367.

[43] J. Wang, X. Yang, and S. Lian, "Influence of Friction Coefficient on Wheel-rail Curve Squeal Noise," *Journal of Mechanical Engineering*, vol. 54, no. 4, p. 255, Jan. 2018, doi: 10.3901/JME.2018.04.255.

[44] X. Feng, G. Chen, Q. Song, B. Dong, and W. Ren, "A Root Cause of Curve Squeal: Self-Excited Frictional Vibration of a Wheelset–Track System," *Journal of Tribology*, vol. 146, no. 6, pp. 1–20, Jun. 2024, doi: 10.1115/1.4064509.

[45] L. E. Buckley-Johnstone, G. Trummer, P. Voltr, K. Six, and R. Lewis, "Full-scale testing of low adhesion effects with small amounts of water in the wheel/rail interface," *Tribology International*, vol. 141, p. 105907, Jan. 2020, doi: 10.1016/j.triboint.2019.105907.

[46] H. Harrison, "Producing and measuring the 3rd body layer," *in 2020 Joint Rail Conference*, Apr. 2020, doi: 10.1115/JRC2020-8095.

[47] Y. A. Areiza, S. I. Garcés, J. F. Santa, G. Vargas, and A. Toro, "Field measurement of coefficient of friction in rails using a hand-pushed tribometer," *Tribology International*, vol. 82, pp. 274–279, Sep. 2014, doi: 10.1016/j.triboint.2014.08.009.

[48] W. J. Wang, P. Shen, J. H. Song, J. Guo, Q. Y. Liu, and X. S. Jin, "Experimental study on adhesion behavior of wheel/rail under dry and water conditions," *Wear*, vol. 271, no. 9–10, pp. 2699–2705, Jul. 2011, doi: 10.1016/j.wear.2011.01.070.

APPENDIX

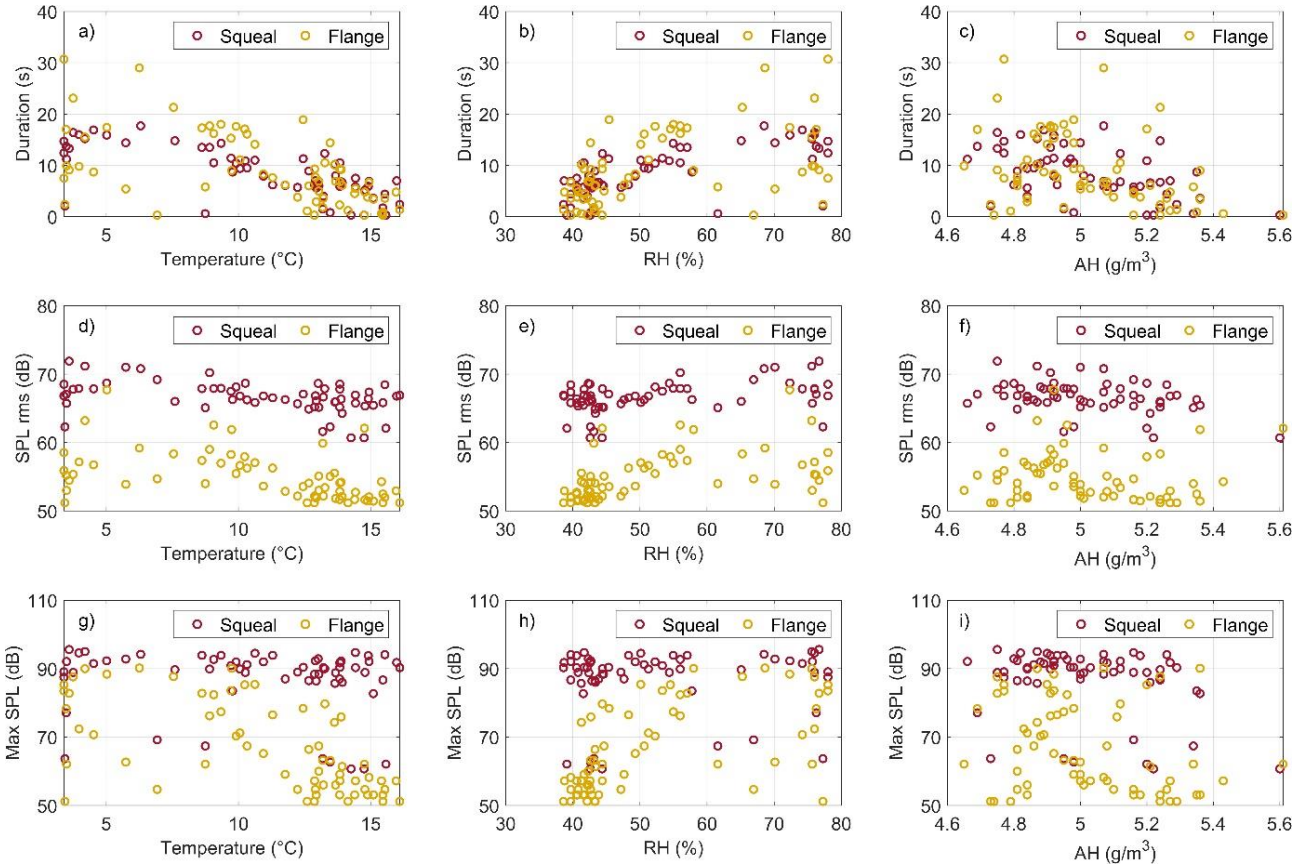

A.1 The effect of temperature, RH and AH on duration, SPL rms and max SPL for squeal and flange noise.